In silico investigation of ligand-regulated palladium-catalysed formic acid dehydrative decomposition under acidic conditions

Chaoren Shen,*[ac] Kaiwu Dong,[a] Zhihong Wei[b] and Xinxin Tian*[b]

[a] Chang-Kung Chuang Institute, Shanghai Key Laboratory of Green Chemistry and Chemical Processes, School of Chemistry and Molecular Engineering, East China Normal University, Shanghai 200062 P. R. China. E-mail: shenchaoren@gmail.com

[b] Institute of Molecular Science, Key Laboratory of Materials for Energy Conversion and Storage of Shanxi Province, Shanxi University, Taiyuan 030006, P. R. China. E-mail: tianxx@sxu.edu.cn

[c] State Key Laboratory for Oxo Synthesis and Selective Oxidation (OSSO), Suzhou Research Institute of LICP, Lanzhou Institute of Chemical Physics (LICP), Chinese Academy of Sciences (CAS), Lanzhou 730000, China

Abstract: *In silico* investigation of ligand-regulated palladium-catalysed formic acid dehydrative decomposition to carbon monoxide under acidic conditions was conducted. Two types of bidentate tertiary phosphine ligands were selected on the basis of previous experimental study. And the promoting effect of *para*-toluenesulfonic acid (PTSA) was specifically investigated. The pyridyl group implanted in py^{t}bpx ligand is found to mainly contribute on enhancing the activity of palladium catalyst. The PTSA promoter displays specific role for regenerating active species and supressing dehydrogenation during Pd-py^{t}bpx/Pd-d^{t}bpx catalysed dehydration process. CO releasing process catalysed by Pd-d^{t}bpx also facilitated by adding PTSA. According to the mechanism hereby supposed, introducing electron-withdrawing substitution at para-position of pyridyl rings may further improve the dehydrative decomposition activity of Pd-py^{t}bpx.

Introduction

Carbonylation reactions constitute a potent tool to manufacture carboxylic acids and their derivatives both in industry and academic organic synthesis.[1-7] In general, the proceeding of carbonylation requires the use of toxic carbon monoxide, which thus usually demands certified high pressure reaction vessels.[8] Therefore, developing non-gaseous CO surrogate for conducting safe and facile-operation carbonylation with stoichiometric amount of CO in common Pyrex glass vessels (e.g., the two-chamber reactor[8] and sealed glass tube) is an important and ongoing research topic in the realm of homogenous catalysis.[9-15] Among these established CO surrogates, formic acid and its derivatives is one kind of versatile atom-

economic C1 source. Different to the decomposition of formic ester or *N*-formyl imides releasing CO in the basic conditions for the carbonylation of aryl or alkyl halides,[16-18] the dehydrative decomposition of HCOOH to CO generally depends on the Morgan reaction using excess strong mineral acid (e.g., excess high-concentration sulfuric acid),[19] which is incompatible to the conditions for most of transition-metal catalysed carbonylation reactions. Moreover, undesired dehydrogenation of HCOOH to CO_2 and H_2, which is more thermodynamically favoured, can facilely occur in the presence of various homogenous transition-metal complex catalysts or heterogeneous catalysts and lead to the reduction of unsaturated bonds.[20] Thus, to avoid this side reaction, acetic anhydride has to be added as the activator for in-situ generating the more active CO source mixed anhydride.[21-24] In 2018, Beller and co-workers achieved the selective CO generation directly from HCOOH under acidic condition by a palladium-catalysed system with bidentate tertiary phosphine ligand bearing pyridyl substituents (py^{t}bpx and pyadbpx), which were derived from 1,2-bis(di-*tert*-butylphosphino) methylbenzene (d^{t}pbx) (Figure 1).[25] The utility of this catalytic system in the autoclave-free hydrocarbonylation of all kinds of alkenes was also demonstrated.[25]

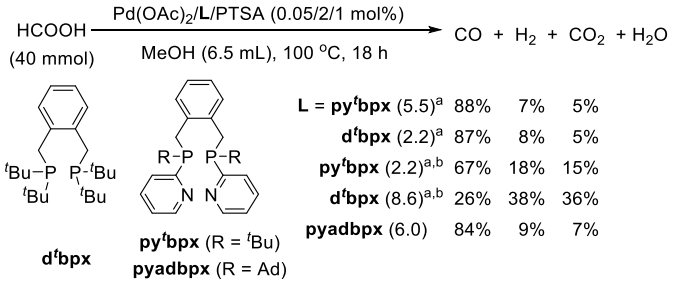

Figure 1. The ligand-regulated palladium-catalysed selective decomposition of HCOOH to CO. PTSA = *para*-toluenesulfonic acid.[25] [a]Molar percentage of gaseous products and in paratheses are total pressure (unit: bar) after reaction. [b]Without adding PTSA. Ad = 1-admantyl.

The experimental investigation by Beller *et al.* disclosed that the activity and selectivity of Pd catalyst to the HCOOH dehydration was regulated by both the ligand and the acid promoter (Figure 1). The ligand py^{t}bpx resulted from replacing two tetra-butyl substituents in d^{t}bpx with 2-pyridyl groups exhibited significantly higher CO selectivity than the original d^{t}bpx ligand (67% *vs*. 26%). Adding catalytic amount of *para*-toluenesulfonic acid (PTSA) can improved the CO selectivity, especially for Pd-d^{t}bpx catalytic system (87% vs. 26%). Meanwhile, the activity towards dehydration using Pd-py^{t}bpx complex is considerably increased (5.5 bar *vs*. 2.2 bar) and higher than that of Pd-d^{t}bpx complex (more detailed results see Figure 1 of ref. 25). The ligand pyadbpx is obtained by further replacing the *tetra*-butyl (^{t}Bu) substituents of py^{t}bpx with bulkier 1-adamantly group (Ad). Pd-pyadbpx catalyst also manifests high activity and selectivity to HCOOH dehydration, which is comparable to the Pd-py^{t}bpx catalyst. These results indicated the importance of "built-in base" (i.e., 2-pyridyl group) in enhancing the activity and selectivity of palladium catalyst.[26] In contrast to the promoting effect of such "built-

in base" on palladium-catalysed hydrocarbonylation of unsaturated hydrocarbons clearly elucidated by the computational survey,[26,27] the explicit role of ligand bearing "built-in base" in palladium-catalysed HCOOH dehydration was yet to be disclosed. Considering that the plausibility of in-situ generated methyl formate acting as CO-releasing agent has been experimentally ruled out[25] (details see Scheme 4 and S1 of ref. 25), we intended to elucidate the role of acid promoter and basic 2-pyridyl group of the ligand in palladium-catalysed formic acid dehydrative decomposition. By density functional theory-based computation, the difference between the Pd-py^{t}bpx and Pd-d^{t}bpx catalysts on the mechanism of formic acid decomposition was revealed.

Computational method

All DFT calculations were performed using Gaussian 16 program.[28] Considering the applicability of meta-generalized gradient approximation (meta-GGA) functional M06[29] on homogeneous organometallic thermochemistry,[30] the M06 functional in conjugation with the def2-SVP basis set[31] was used for structure optimization. Corresponding frequency calculation using the same method was done to characterize the nature of the optimized structures, i.e., energy minimums without imaginary frequencies or transition states with only one imaginary frequency. Intrinsic reaction coordinate (IRC) was used to check the imaginary model that connects the initial and the final states. In addition, we used M06 in conjugation with the def2-TZVP basis set to conduct the self-consistent reaction field (SCRF) single-point calculations based on the M06/def2SVP-optimized geometries by using the SMD solvation model[32] and methanol as solvent to Gibbs free energies (M06-SCRF/def2-TZVP//M06/def2-SVP). The thermal corrections to Gibbs free energy at 373 K calculated by the Shermo program[33] were added to the total electronic energies from the SCRF single-point energy calculations. The corrected Gibbs free energy (ΔG) at 373 K were therefore used in the following discussion and comparison.

Results and discussion

HCOOH dehydration by Pd-py^{t}bpx or Pd-d^{t}bpx (paths A-D)

Experimental results have demonstrated that the presence of PTSA is critical to the activity and selectivity of Pd-catalysed dehydration of HCOOH.[25] Thus, two sets of mechanism with or without the aid of PTSA promoter were considered for this process. A previous study has revealed that the nitrogen atom of the pyridyl ring has a higher proton affinity than the palladium atom in the acidic conditions,[26,27] similar trend is also found in this study. Therefore, the coordination-unsaturated cationic Pd^0-py^{t}bpx complex **1-py^{t}bpx** bearing protonated pyridyl group is regarded as the active species for Pd-py^{t}bpx catalyst and the starting point of reaction course, while the zero-valent palladium complex **1-d^{t}bpx** is chosen as the active species for Pd-d^{t}bpx catalyst. And the oxidative addition of HCOOH to Pd(0) is supposed as the first step. The

coordination between HCOOH and **1-py^{t}bpx** or **1-d^{t}bpx** affording coordination-saturated palladium complex is moderately endothermic (2.9-5.3, 7.3-9.5 kcal/mol, respectively). Detailed free-energy changes see Fig. S1 in SI. The plausible coordination of methanol solvent to the Pd(0) centre is also considered. The coordination of CH_3OH to **1-py^{t}bpx** is more endothermic (8.9 kcal/mol, Fig. S1) than that of HCOOH, and the structure of CH_3OH-coordinated **1-d^{t}bpx** cannot be located. These results further rationalize the initial active species adopted in this work. Given that CH_3OH can form complex hydrogen-bonding interaction network with HCOOH, PTSA or itself and water by-product is gradually accumulated in the course of HCOOH dehydration, the explicit solvation of CH_3OH and H_2O are omitted to simplify the reaction model and only the implicit solvation of CH_3OH is considered in this computational investigation.

Fig. 2 illustrated the two plausible paths for HCOOH dehydration to CO catalysed by Pd-py^{t}bpx (path **A** and **B**). Path **A** starts from the C-H activation of HCOOH by **1-py^{t}bpx** (HCOOH + **1-py^{t}bpx** → **2-py^{t}bpx** via **TS1-py^{t}bpx**) followed by the intramolecular dehydration facilitated by the pyridinium group (**2-py^{t}bpx** → **3-py^{t}bpx** + H_2O via **TS2-py^{t}bpx**). The first step is endergonic by 10.3 kcal/mol, with a barrier of 12.3 kcal/mol. The generated **2-py^{t}bpx** has an intramolecular hydrogen-bonding between the OH of COOH group and the proton attaching to the nitrogen atom of pyridyl group. The directly combination of OH and (N-)H and subsequent delivering one H_2O molecule has low barrier of 11.6 kcal/mol and is highly exergonic by 17.6 kcal/mol. Considering the co-existence of PTSA, HCOOH and CH_3OH in the catalytic system, PTSA-, HCOOH- or CH_3OH-involved processes are also investigated. Oppositely, inserting HCOOH, PTSA or MeOH into this intramolecular hydrogen bond and forming a seven-membered ring connected by two hydrogen bonds is thermodynamically unbeneficial (detailed result see Fig. S2 in SI). We therefore suppose that the dehydration step has no PTSA, MeOH or the second HCOOH molecule involved. Afterwards, the carbonyl palladium hydride complex **3-py^{t}bpx** can directly release CO with the formation of palladium hydride complex **4b-py^{t}bpx** followed by the direct hydrogen migration of **4b-py^{t}bpx** to recover **1-py^{t}bpx** via **TS3b-py^{t}bpx**. As shown in Fig. 2, the decarbonylation process is highly endergonic by 29.7 kcal/mol, but the hydrogen migration is almost barrierless. With the assistance of PTSA, HCOOH or CH_3OH, it is found that although the ligand exchange with these three species is all endergonic, the three intermediates **4-py^{t}bpx**, **4a-py^{t}bpx** and **4c-py^{t}bpx** are all thermodynamically more stable than the **4b-py^{t}bpx** (1.5, 4.1, 4.6 vs. 22.4 kcal/mol). And the apparent Gibbs free energies of **TS3-py^{t}bpx** and **TS3a-py^{t}bpx** are lower than that of **TS3b-py^{t}bpx** (15.5, 16.1 vs. 20.3 kcal/mol), while the Gibbs free energy of **TS3c-py^{t}bpx** is much higher than that of **TS3b-py^{t}bpx** (34.3 vs. 20.3 kcal/mol). Therefore, we can deduce that PTSA- and HCOOH-assisted hydrogen migration processes are both possible. The detailed processes are compared in Fig.3. It is noticed that the further protonation of **3-py^{t}bpx** by PTSA and the following CO dissociation as well as the **1-py^{t}bpx** regeneration steps are more

thermodynamically beneficial than that of by HCOOH. Also, the Gibbs free energy of **TS3-py^{t}bpx** is 0.6 kcal/mol lower than that of **TS3a-py^{t}bpx**. All these suggest that adding PTSA indeed facilitate the CO releasing and catalyst regeneration.

Path **B** also starts from the C-H activation of HCOOH by **1-py^{t}bpx** (HCOOH + **1-py^{t}bpx** → **2a-py^{t}bpx** via **TS1a-py^{t}bpx**). Differently, the intramolecular hydrogen-bonding in **TS1a-py^{t}bpx** and **2a-py^{t}bpx** lies between the oxygen atom of carbonyl group and the H-N moiety of pyridinium group. When **2a-py^{t}bpx** undergoes the intermolecular dehydration to **3a-py^{t}bpx** facilitated by PTSA or HCOOH as the proton shuttle, the barrier via **TS2a-py^{t}bpx**/**TS2b-py^{t}bpx** containing eight-membered proton transfer ring is lower than that via **TS2d-py^{t}bpx**/**TS2e-py^{t}bpx** both containing six-membered proton transfer ring (46.1/39.0 vs. 49.5/48.3 kcal/mol). The afforded H_2O comes from the combination of OH group of COOH and the proton of acid, while the hydrogen atom binding to Pd centre is transferred to the oxygen terminal of acid. In the absence of both PTSA and HCOOH, the subsequent intramolecular dehydration of **2a-py^{t}bpx** squeezing out one H_2O molecule via **TS2c-py^{t}bpx** also needs to surmount the energy barrier of high as 39.9 kcal/mol. The formed H_2O comes from the combination between the OH group of COOH and the H atom connecting to Pd. Finally, **1-py^{t}bpx** is regenerated from the decarbonylation of **3a-py^{t}bpx**, which is strongly endothermic by 19.8 kcal/mol. It can be seen that HCOOH-assisted dehydration via **TS2b-py^{t}bpx** has close barrier with the direct dehydration process via **TS2c-py^{t}bpx** (39.0 vs. 39.9 kcal/mol), while PTSA-mediated dehydration has higher barrier (46.1 kcal/mol).

The obtained free-energy results about path **A** and **B** revealed the dehydration step (**2-py^{t}bpx** → **TS2-py^{t}bpx** and **2a-py^{t}bpx** → **TS2b-py^{t}bpx**) is the rate-degerming step in both paths. However, the free energy of **TS2-py^{t}bpx** is evidently much lower than that of **TS2b-py^{t}bpx** (21.9 vs. 48.7 kcal/mol). Suggesting that the protonated pyridyl group directly attends the dehydration process by contributing its own proton can drastically reduce the apparent activation energy of HCOOH dehydration to CO. Moreover, in the absent of PTSA, HCOOH-assisted CO releasing and catalyst regeneration process is favourable. Adding PTSA can considerably promote the CO dissociation from intermediate **3-py^{t}bpx** and the regeneration of active species **1-py^{t}bpx**.

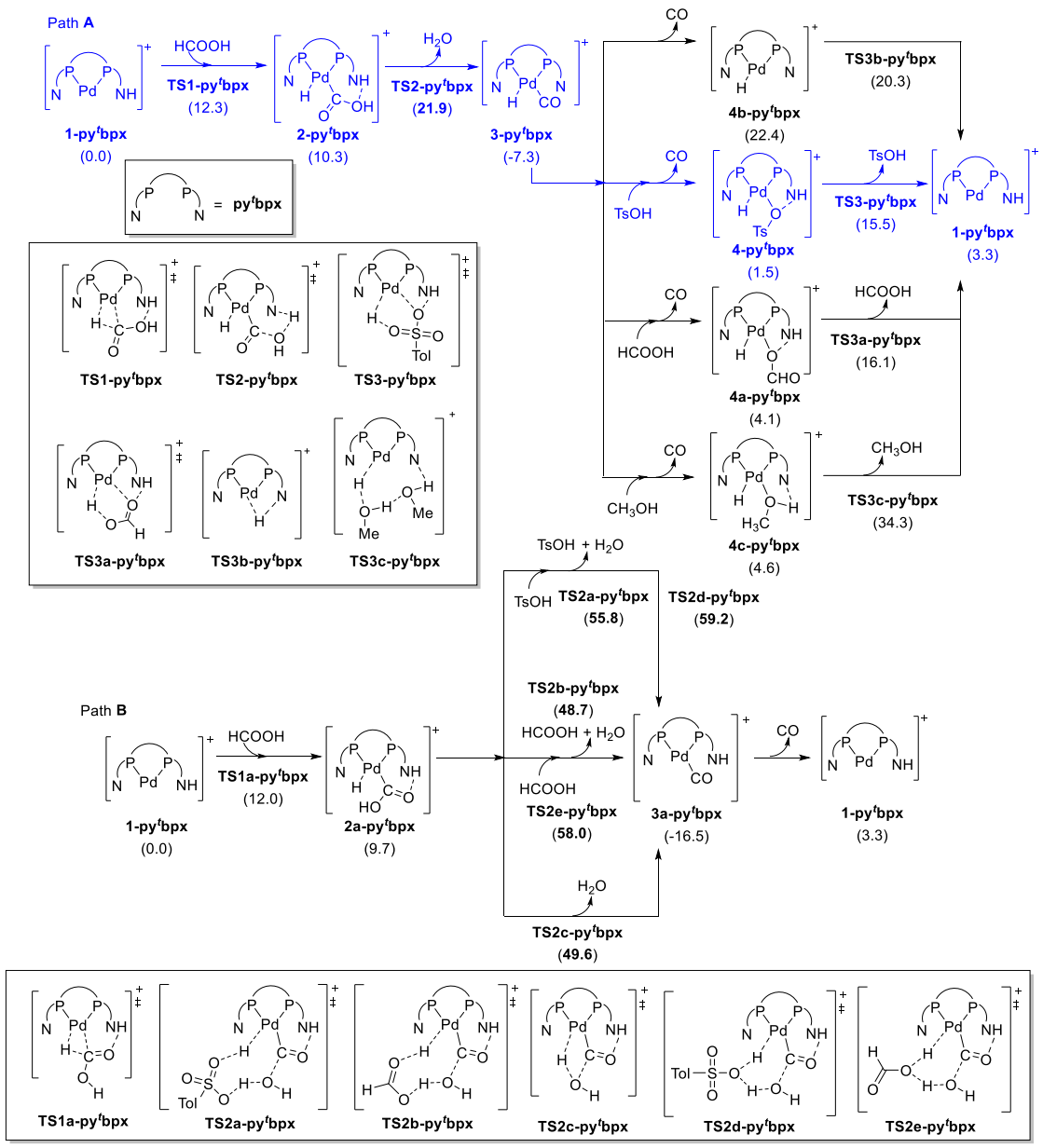

Figure 2. The dehydration of HCOOH catalysed by Pd-py^{t}bpx (path **A** and **B**).

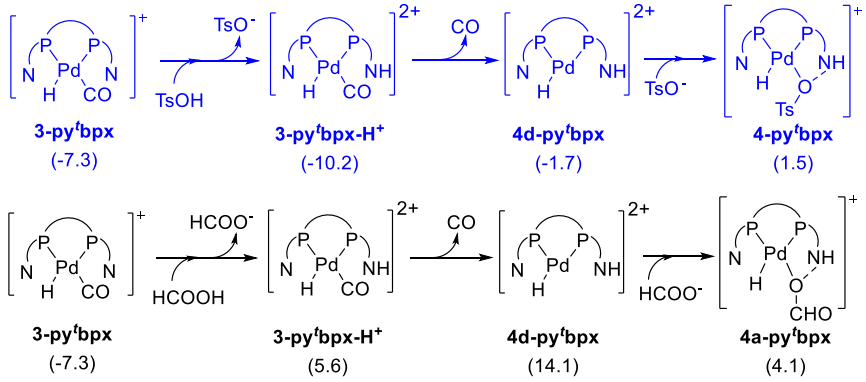

Figure 3 Detailed process and free-energy changes for the CO dissociation and ligand exchange of **3-py^{t}bpx** to **4-py^{t}bpx** and **4a-py^{t}bpx** respectively by PTSA and HCOOH.

Figure 4 displays the two plausible paths (path **C** and **D**) for HCOOH dehydration catalysed by Pd-d^{t}bpx (**1-d^{t}bpx**). Similar to the dehydration by Pd-py^{t}bpx, path **C** and **D** are also initiated from the C-H activation of HCOOH with **1-py^{t}bpx** (HCOOH + **1-d^{t}bpx** → **2-d^{t}bpx** via **TS1-d^{t}bpx**). The process is endergonic by 12.1 kcal/mol, with a barrier of 14.9 kcal/mol. The further transformation of **2-d^{t}bpx** has two alternatives: i) the acid directly-participated intermolecular dehydration to afford the carbonyl palladium hydride intermediate **3-d^{t}bpx** (path **C**); ii) the acid-assisted intermolecular dehydration or direct intramolecular dehydration to give the carbonyl palladium intermediate **3a-d^{t}bpx** (path **D**).

In path **C**, the PTSA-mediated intermolecular dehydration via **TS2-d^{t}bpx** exhibited significantly lower energy barrier than the HCOOH-mediated process via **TS2a-d^{t}bpx** (11.7 vs. 17.6 kcal/mol). The former process to **3-d^{t}bpx** is much more exothermic than the latter one (-30.6 vs. -14.8 kcal/mol). Thus, the transformation from **2-d^{t}bpx** to **3-d^{t}bpx** via **TS2-d^{t}bpx** is both kinetically and thermodynamically more favoured. For the PTSA- and HCOOH-attended intermolecular dehydration of **2-d^{t}bpx**, we also obtained the transition states **TS2e-d^{t}bpx** and **TS2f-d^{t}bpx** bearing six-membered ring motif for transferring proton from the acid onto the OH group. But both have much higher free energy than **TS2-d^{t}bpx** and **TS2a-d^{t}bpx**, respectively (details see Fig. S3 in SI). Intermediate **4-d^{t}bpx** generated from the ligand exchange between carbonyl of **3-d^{t}bpx** and free *para*-toluenesulfonate anion is also more stable than **4a-d^{t}bpx** afforded from the ligand exchange between carbonyl ligand of **3-d^{t}bpx** and free formate anion. In the final step for regenerating **1-d^{t}bpx**, the location of **TS3-d^{t}bpx** on the free energy surface is 2.8 kcal/mol lower than that of **TS3a-d^{t}bpx**.

In path **D**, the intermolecular dehydration to **3a-d^{t}bpx** with the mediation of PTSA or HCOOH as proton shuttle via **TS2b-d^{t}bpx** and **TS2c-d^{t}bpx** both bearing eight-membered proton transfer chain requires to overcome the energy barrier of 13.8 or 18.7 kcal/mol. In comparison, the acid-absent intramolecular dehydration of **2-d^{t}bpx** to **3a-d^{t}bpx** via **TS2d-d^{t}bpx** requires to overcome the energy barrier as high as 37.8 kcal/mol. Moreover, the decarbonylation of **3a-d^{t}bpx** to regain **1-d^{t}bpx** and produce CO gas is endoergic by 15.3 kcal/mol. Although the acid-mediated intermolecular dehydration in path **D** has moderate energy barrier, the lower free energy of **TS2-d^{t}bpx** than **TS2b-d^{t}bpx** by 2.1 kcal/mol suggests that PTSA-mediated path **C** is more advantageous than PTSA-mediated path **D**. However, in the absent of PTSA, the HCOOH-assisted path **C** is kinetically favourable than the HCOOH-assisted or non-assisted path **D** (29.7 vs. 30.8/49.9 kcal/mol).

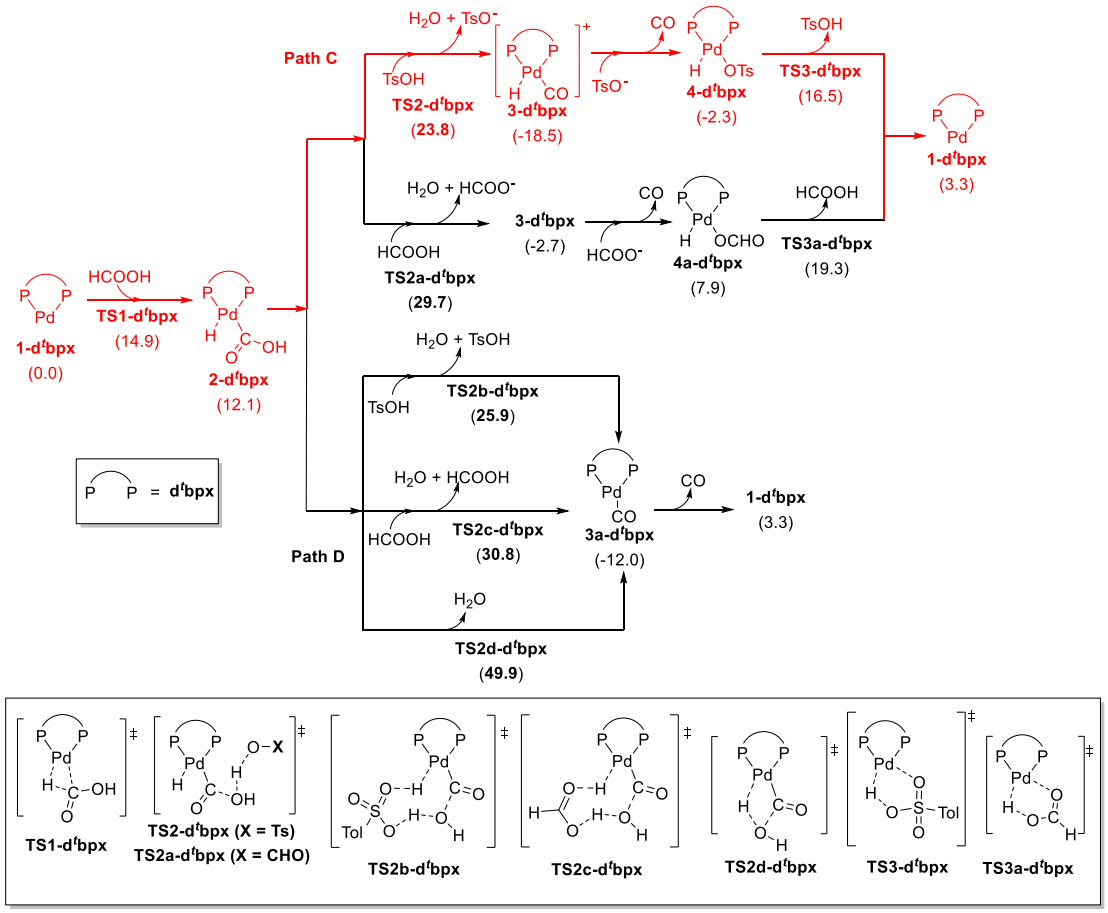

Figure 4. The dehydration of HCOOH catalysed by Pd-d^{t}bpx (path **C** and **D**).

Since the C-O bond activation of HCOOH intermediate by heterogeneous catalysts is one key step of water-gas shift reaction,[34] the possibility of dehydration beginning with the C-O bond cleavage of HCOOH by **1-py^{t}bpx**/**1-d^{t}bpx** affording **2b-py^{t}bpx**/**2a-d^{t}bpx** has also been estimated. Opposite to breaking off C-H bond, the C-O bond cleavage of HCOOH by **1-py^{t}bpx** or **1-d^{t}bpx** needs to overcome much higher energy barrier and much more endoergic (Figure 5). Barrier for the C-O bond cleavage of HCOOH by **1-py^{t}bpx**/**1-d^{t}bpx** via **TS1b-py^{t}bpx**/**TS1a-d^{t}bpx** is high as 30.8/31.6 kcal/mol and this transformation also highly endothermic by more than 30 kcal/mol. This energy pattern has clearly indicated that the HCOOH dehydration initialized with the activation of C-O bond is much less probable under such relatively low reaction temperature. Thus, the subsequent intramolecular dehydration or acid-mediated intermolecular dehydration of **2b-py^{t}bpx**/**2a-d^{t}bpx** is not further discussed.

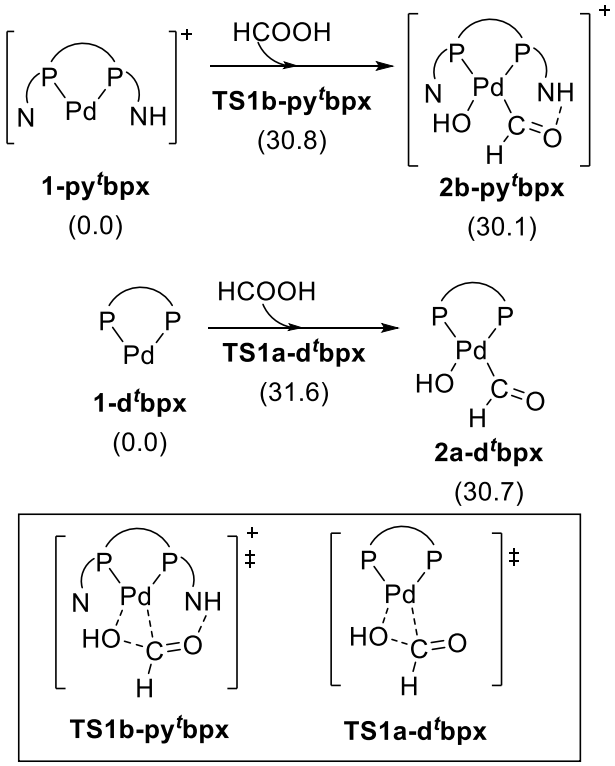

Figure 5. The C-O bond cleavage of HCOOH by Pd-py^{t}bpx or Pd-d^{t}bpx.

When using the complex of Pd-d^{t}bpx as the catalyst, the possibility of cationic palladium hydride complex **4c-d^{t}bpx** generated from the oxidation of **1-d^{t}bpx** by PTSA or HCOOH is also concerned. The obtained results show that the generation of **4c-d^{t}bpx** in the presence of PTSA is thermodynamically and kinetically favoured (Fig. S4 in SI). In contrast, generating **4c-d^{t}bpx** from the oxidation of **1-d^{t}bpx** by HCOOH in the absence of PTSA is not facilitated. Thus, the existence of **4c-d^{t}bpx** is only reasonable when PTSA is added. We further considered the dehydration of HCOOH by **4c-d^{t}bpx**. The computation result revealed that energy barrier for the dehydration of HCOOH by **4c-d^{t}bpx** via **TS1b-d^{t}bpx** giving palladium-formyl complex **2b-d^{t}bpx** is high as 46.1 kcal/mol (Fig. 6), although the following exothermic decomposition of **2b-d^{t}bpx** to **4d-d^{t}bpx** is barrierless and regeneration of **4c-d^{t}bpx** from **4d-d^{t}bpx** is mildly endothermic. In comparsion, the palladium hydride complex **4c-d^{t}bpx** undergoing deprotonation firstly to Pd(0) complex **1-d^{t}bpx** (endothermic by 10.7 kcal/mol), and then following the pathway **A** to release CO has the apparent barrier 34.5 kcal/mol, which is still far lower than the 46.1 kcal/mol. Therefore, we think that treating the Pd(0) complex **1-d^{t}bpx** as the active species is more rational than the cationic palladium hydride complex **4c-d^{t}bpx** in this reaction course. Hence, the dehydrogenative side-reaction by **4c-d^{t}bpx** is not included in the following discussion.

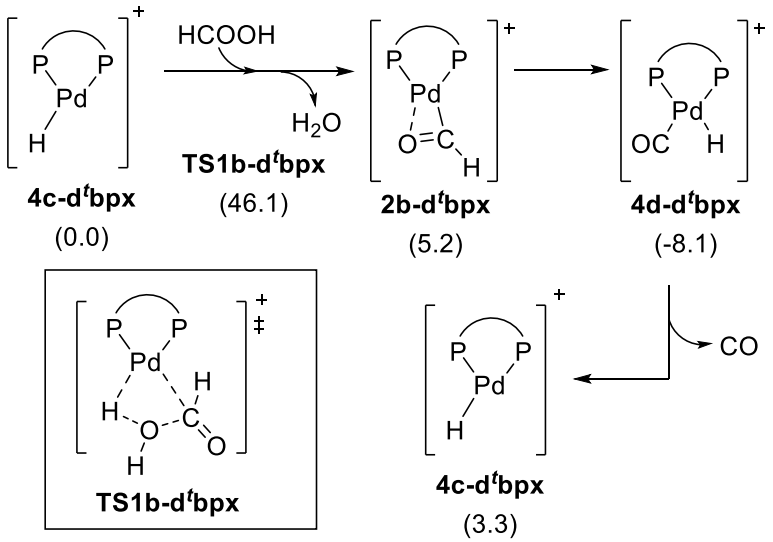

Figure 6. The dehydration of HCOOH by the coordination-unsaturated cationic palladium hydride complex **4c-d^{t}bpx**.

HCOOH dehydrogenation by Pd-py^{t}bpx or Pd-d^{t}bpx (path E, F, G and H)

As the side reaction during the dehydration of HCOOH, the HCOOH dehydrogenation to H_2 and CO_2 by Pd-py^{t}bpx (Fig. 7) or Pd-d^{t}bpx (Fig. 8) has two plausible paths. The paths start from cleaving the different bonds of HCOOH.

Path **E/G** undergoes a two-step process starting from the C-H activation of HCOOH by **1-py^{t}bpx** or **1-d^{t}bpx** followed by the dehydrogenative decomposition of **2a-py^{t}bpx** and **2-d^{t}bpx** yielding H_2 and CO_2. Similar to the scenario in the dehydration, the dehydrogenation of **2a-py^{t}bpx** and **2-d^{t}bpx** also have three different channels: PTSA- or HCOOH-mediated intermolecular dehydrogenation correspondingly via **TS4a** and **TS4b**, as well as the direct intramolecular dehydrogenation via **TS4**. As shown in Fig.7 and 8, in path **E**/**G**, the dehydrogenation step is the rate-determining step, and the acid-assisted intermolecular dehydrogenation is energetically more favoured than the direct intramolecular dehydrogenation. For Pd-py^{t}bpx, the free energy of **TS4b-py^{t}bpx** is about 2.2 kcal/mol lower than **TS4-py^{t}bpx** and **TS4a-py^{t}bpx**. However, for Pd-d^{t}bpx, the free energy of **TS4a-d^{t}bpx** is much lower than **TS4-d^{t}bpx** and **TS4b-d^{t}bpx**. Path **F/H** undergoes a four-step process starting from breaking off the O-H bond of HCOOH by **1-py^{t}bpx** or **1-d^{t}bpx** followed by the decarboxylative decomposition of **4e-py^{t}bpx** and **4a-d^{t}bpx** to release CO_2 and afford palladium dihydride complex **5-py^{t}bpx** and **5-d^{t}bpx**. Finally, H_2 is produced via the reductive elimination of **5-py^{t}bpx** and **5-d^{t}bpx**. For both catalysts, the decarboxylation is the rate-determining step of path **F**/**H**. Comparing with path **E/G**, the apparent reaction barrier of path **F**/**H** is much lower (18.2/17.2 kcal/mol *vs.* 34.4/31.3 kcal/mol). Thus, the dehydrogenation proceeding along path **F**/**H** is more facile than path **E**/**G**. Noteworthily, the decarboxylation of **4e-py^{t}bpx** and **4a-**

d^{t}bpx can be evidently impeded by the exoergic protonation of **4e-py^{t}bpx** and **4a-d^{t}bpx** by PTSA delivering **4f-py^{t}bpx** and **4b-d^{t}bpx** (-5.2 and -8.7 kcal/mol). Oppositely, the protonation of **4e-py^{t}bpx** and **4a-d^{t}bpx** by HCOOH giving **4f-py^{t}bpx** and **4b-d^{t}bpx** is endothermic by 10.6 and 7.1 kcal/mol. For the complex of **py^{t}bpx** ligand, with or without adding PTSA, **4f-py^{t}bpx** can be easily recovered to **1-py^{t}bpx** (Fig. 7). The energy barrier for this process is 12.2 or 12.8 kcal/mol, much lower than the apparent reaction barrier of path **F** (18.2 kcal/mol). In other words, the reaction course after cleaving the O-H bond of HCOOH can easily fall into the proton exchange with HCOOH or PTSA, which leads to the prohibition of H_2 releasing. For **d^{t}bpx** ligand complex, the energy barrier for **4b-d^{t}bpx** recovered to **1-d^{t}bpx** is 13.2 kcal/mol when PTSA is present, which is lower than the apparent reaction barrier of path **H** (17.2 kcal/mol). Without PTSA, the apparent energy barrier for recovering **1-d^{t}bpx** from **4b-d^{t}bpx** by the proton exchange with the other HCOOH molecule is 16.0 kcal/mol. This value is very close to the barrier of H_2 releasing, which suggests that there may be a quick equilibrium between these two reaction courses. The results well explain the lower H_2/CO_2 selectivity of **Pd-py^{t}bpx** complex with or without adding PTSA and **Pd-d^{t}bpx** complex with adding PTSA.

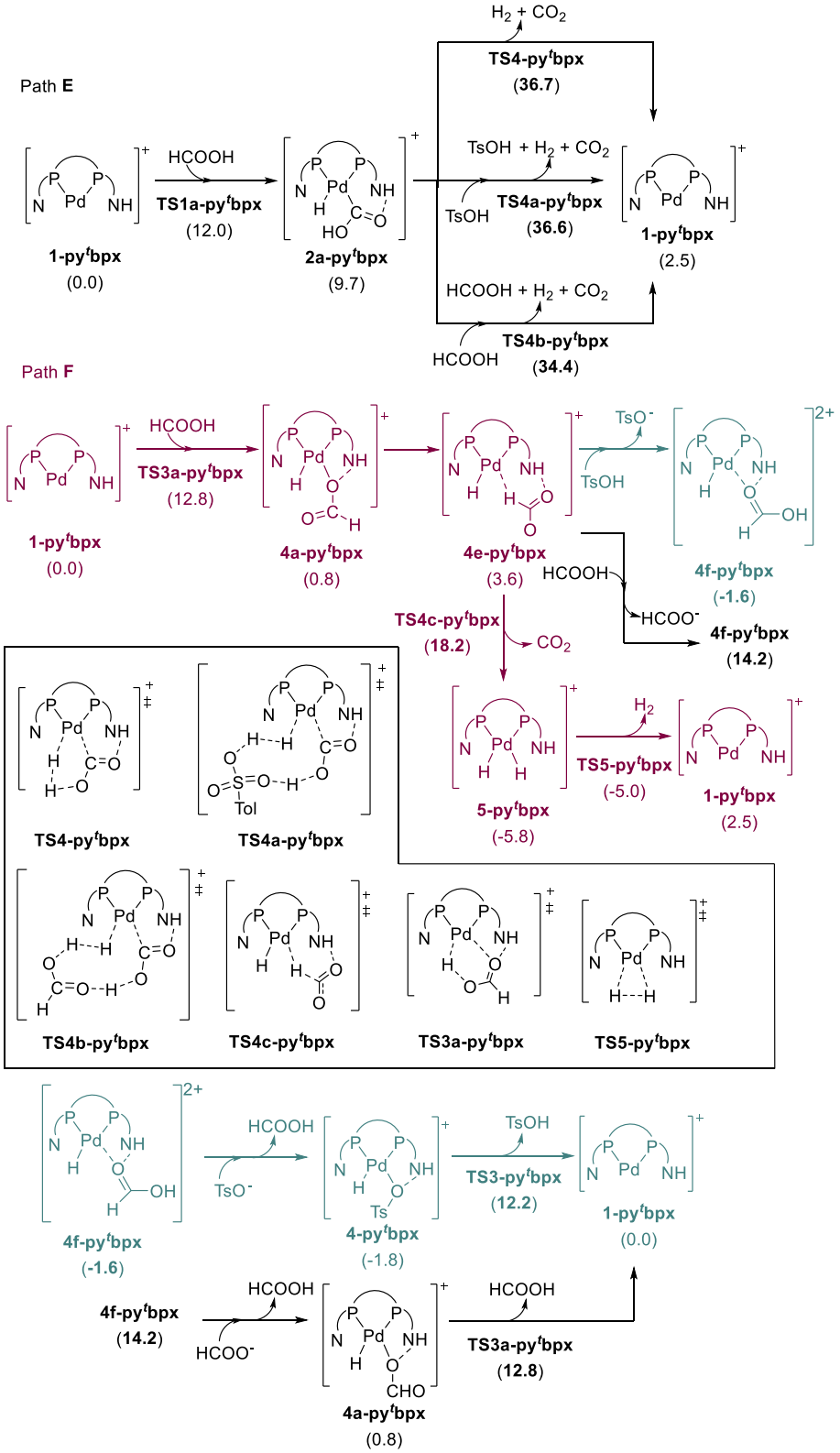

Figure 7 The dehydrogenation of HCOOH catalysed by Pd-py^{t}bpx (path **E** and **F**)

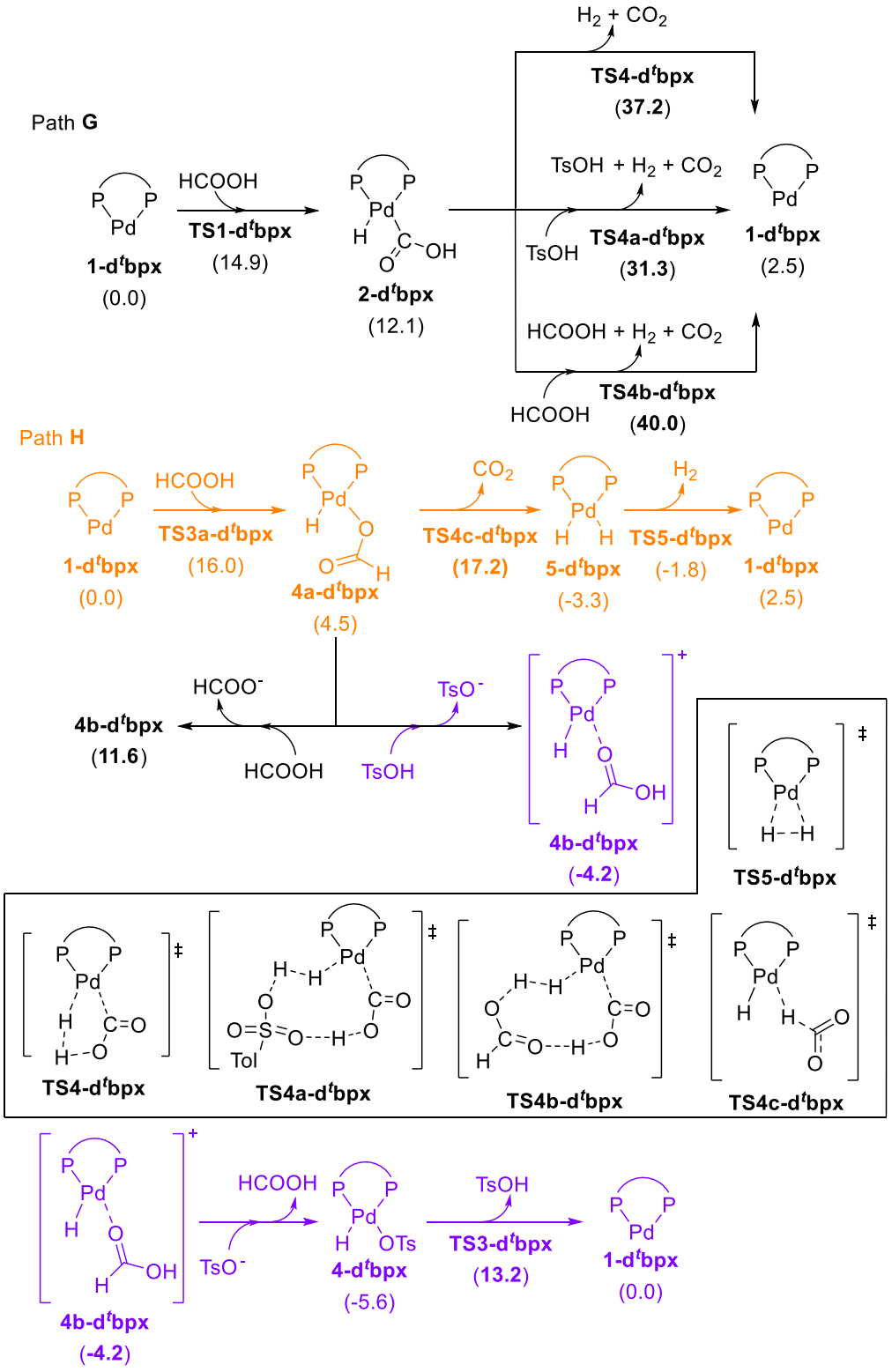

Figure 8 The dehydrogenation of HCOOH catalysed by Pd-d^{t}bpx (path **G** and **H**)

Free energy comparison between different paths

The free-energy changes for CO releasing and dehydrogenation pathways by Pd-py^{t}bpx and Pd-d^{t}bpx catalysts are compared in Scheme 1. In the absence of PTSA, the highest point of the

free energy surface for Pd-py^{t}bpx and Pd-d^{t}bpx catalysed HCOOH dehydration releasing CO is **TS2-py^{t}bpx** and **TS2a-d^{t}bpx**, respectively. Obviously, Pd-py^{t}bpx catalyst has lower barrier for CO releasing (21.9 vs 29.7 kcal/mol). With PTSA assisted, the regeneration of active catalyst in the reaction course of HCOOH dehydration is promoted by PTSA, while the dehydration step keeps still. Importantly, the free energy of **TS2-py^{t}bpx** still lower than **TS2-d^{t}bpx** by 1.9 kcal/mol (21.9 vs 23.8 kcal/mol), this clearly manifests that the intramolecular dehydration by the protonated "built-in base" in py^{t}bpx ligand validly improves the catalytic efficiency of palladium catalyst in the dehydration of HCOOH to CO. Moreover, the lower free energy of **TS1-py^{t}bpx** than **TS1-d^{t}bpx** by 2.6 kcal/mol discloses that the presence of hydrogen-bonding interaction between HCOOH and the protonated py^{t}bpx ligand significantly mitigates the energy barrier for the C-H bond cleavage of HCOOH and stabilizes the intermediate **2-py^{t}bpx**. The apparent reaction barrier for the dehydrogenation process by Pd-py^{t}bpx/Pd-d^{t}bpx along path **F**/**H** (18.2/17.2 kcal/mol) is much lower than the dehydration by Pd-py^{t}bpx/Pd-d^{t}bpx along path **A**/**C**. However, the intermediate **4e-py^{t}bpx/4a-d^{t}bpx** prefers to be transformed to the active catalyst rather than releasing CO_2, which inhibits the H_2 production indirectly. Compared to the scenario without PTSA, adding PTSA has slight effect on mitigating the barrier of recovering **1-py^{t}bpx** from **4e-py^{t}bpx**. However, it can considerably reduce the barrier of regenerating the active catalyst **1-d^{t}bpx** from **4a-d^{t}bpx**. That's to say, adding PTSA does not change the dehydrogenation activity of **1-d^{t}bpx**, but makes the regeneration of **1-d^{t}bpx** diverging from the reaction course of dehydrogenation more competitive than H_2 production, and therefore inhibits the H_2/CO_2 production.

For Pd-py^{t}bpx, PTSA improves the activity only by facilitating the CO dissociation and the regeneration of active species, while the pyridinium group contributes more to other steps. The calculated results of Pd-py^{t}bpx catalyst well explain the high and stable chemoselectivity to CO by Pd-py^{t}bpx under the PTSA-absent conditions. For Pd-d^{t}bpx, adding PTSA can enhance the activity of dehydration and diminish the dehydrogenation, which significantly changes the relative selectivity. When adding PTSA promoter, the apparent CO releasing barrier of Pd-py^{t}bpx is lower than that of Pd-d^{t}bpx (21.9 vs. 23.8 kcal/mol), indicating the higher activity of Pd-py^{t}bpx catalyst, which also in line with the experimental observation. It also should be mentioned that the recently reported computational investigation on producing CO from methyl formate intermediate by Pd-d^{t}bpx suggests a reaction path with apparent energy barrier over 30 kcal/mol,[35] which is much higher than the value obtained in this work. That report partially rationalizes the mechanism proposed in this work. It also should be mentioned that, in sharp contrast to the observed remarkable stability of Pd-py^{t}bpx catalyst,[25,36,37] the catalyst of Pd-d^{t}bpx is always prone to decompose under heating conditions, which leads to the formation of Pd nanoparticles (i.e., Pd black),[36,38] despite that the presence of PTSA can more or less alleviate the decomposition of palladium complex. Such distinction on stability is more obvious under the water-contained acidic conditions.[36,38] Since palladium nanoparticle has high activity and

selectivity towards dehydrogenation of HCOOH even under low temperature,[39-42] we therefore infer that the dehydrogenation during the whole decomposing process of HCOOH catalysed by Pd-d^{t}bpx, is probably partially contributed by the palladium nanoparticle resulted from the degradation of Pd-d^{t}bpx catalyst. Furthermore, the catalytic activity of Pd nanoparticles is susceptible to the particle size, surface structure, oxidation state of Pd atom and pH value of reaction medium.[43-45] Thus, the Pd-d^{t}bpx catalyst system is far more complicated and cannot be simply explained by only considering the single catalyst that studied in this report.

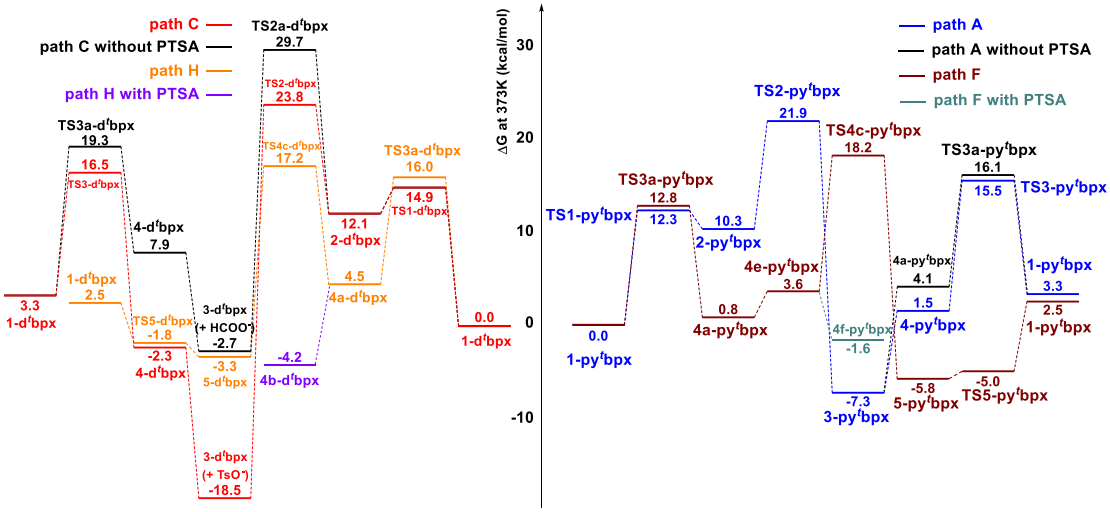

Scheme 1 The solvated free-energy changes of advantaged CO releasing or dehydrogenation pathways for Pd-py^{t}bpx and Pd-d^{t}bpx catalyst at 373 K with or without PTSA promoter (the reaction course along path **F**/**H** with PTSA after **4f-py^{t}bpx**/**4b-d^{t}bpx** was omitted for the clarity of presentation).

Path A and F of Pd-py^{t}bpx in the presence of excess PTSA

Since the molar amount of PTSA is excessive to py^{t}bpx ligand in the experimental report and the further protonation of **1-py^{t}bpx** by PTSA is found to be exothermic (results see Fig. S4 in SI), the scenario of dehydration and dehydrogenation along path **A** and **F** by **1-(py^{t}bpx-H)**, the dicationic palladium catalyst of bis-protonated py^{t}bpx ligand, was also investigated and compared with the paths by **1-py^{t}bpx**. Fig. 9 summarizes the overall process of path **A** and **F** by **1-(py^{t}bpx-H)**. The apparent barriers of HCOOH dehydration and dehydrogenation respectively along path **A** and **F** by **1-(py^{t}bpx-H)** are elevated to 27.1 and 28.9 kcal/mol. The energy barriers for cleaving the C-H and O-H bonds of HCOOH by **1-(py^{t}bpx-H)** in path **A** and **F** also go up to 17.1 and 17.4 kcal/mol, respectively. Moreover, owing to the presence of two hydrogen-bonding interaction between the coordinated formate anion and the bis-protonated py^{t}bpx ligand, the transformation from **4a-(py^{t}bpx-H)** to **4d-(py^{t}bpx-H)** is far more endothermic than the corresponding transformation from **4a-py^{t}bpx** to **4d-py^{t}bpx**. The presence of PTSA also inhibits the decarboxylation of **4d-(py^{t}bpx-H)** by protonating **4d-**

(py^{t}bpx-H) to **4e-(py^{t}bpx-H)**. The energy barrier for recovering **1-(py^{t}bpx-H)** from **4e-(py^{t}bpx-H)** is lower than the apparent reaction barrier of path **F**. In short, the further protonation of **1-py^{t}bpx** by PTSA reduces the activity of Pd-py^{t}bpx catalyst on both dehydration and dehydrogenation. Meanwhile, the apparent barrier of path **F** exceeds over that of path **A**, which makes the chemoselectivity of catalyst more favoured to HCOOH dehydration. This is also in line with the experimental report.[25]

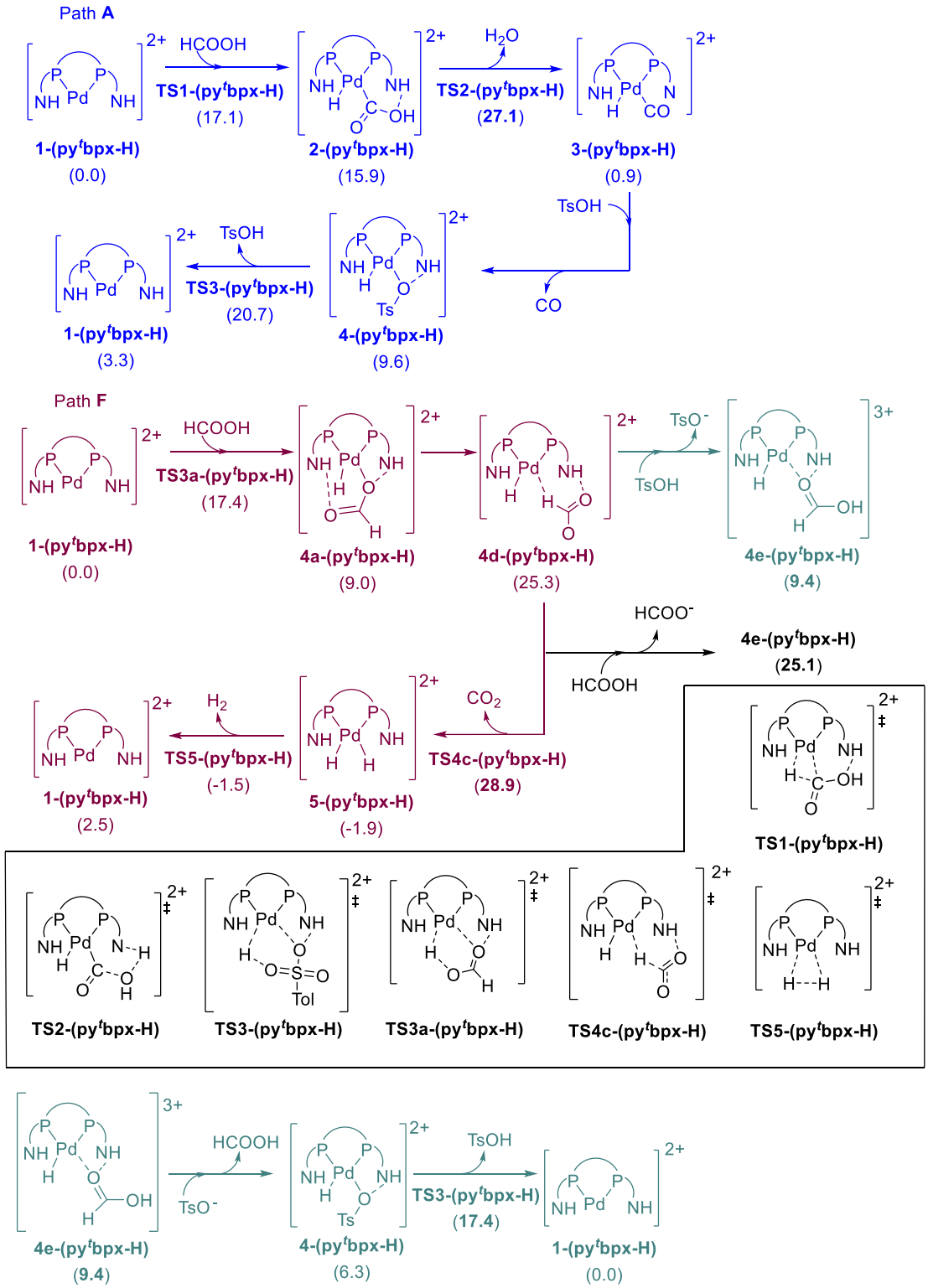

Figure 9. Free-energy changes for path **A** and **F** by the bis-protonated Pd-py^{t}bpx catalyst.

Preliminary survey and prediction of the structure-activity relationship between ligand and PTSA-mediated HCOOH dehydration

The preliminary survey and prediction on the relationship between the structure of phosphine ligand based on the skeleton of py^{t}bpx and the activity of PTSA-mediated HCOOH dehydration was also conducted. Since Pd-pyadbpx catalyst exhibits slightly higher activity than Pd-py^{t}bpx in the PTSA-promoted HCOOH dehydration (Fig. 1), the reaction proceeding along path **A** catalysed by Pd-pyadbpx was computed to reveal the effect of more sterically hindered 1-adamantyl group on each elementary step. Fig. 10 demonstrated that compared with the corresponding transition states in path **A** by Pd-py^{t}bpx, introducing 1-admantyl group into the pyridyl-substituted bidentate phosphine ligand leads to the drop on the free energy of **TS1** and **TS2** as well as the mitigation of apparent energy barrier (20.8 vs. 21.9 kcal/mol) for overall process. Meanwhile, the free energy of **TS3** for regenerating **1-pyadbpx** is elevated. The obtained overall energy profile for PTSA-mediated HCOOH dehydration by Pd-pyadbpx is in line with the aforementioned experimental observation.

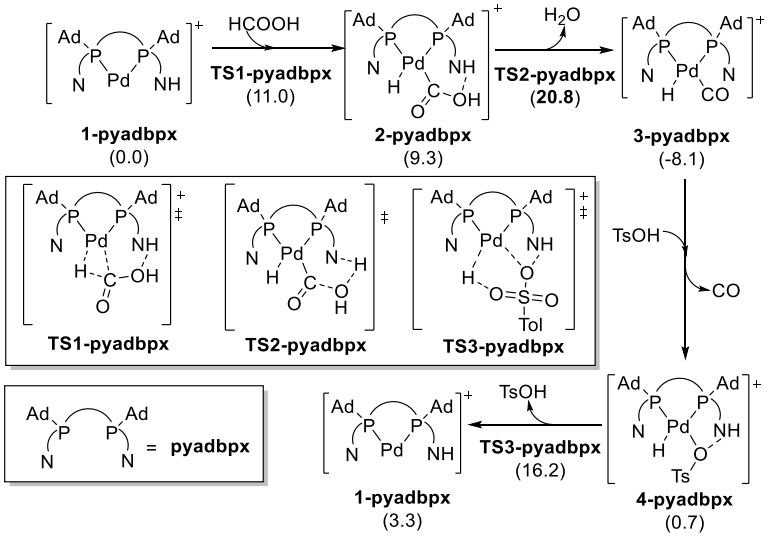

Figure 10. Free-energy changes for HCOOH dehydration by Pd-pyadbpx catalyst along path **A**

Since the intramolecular dehydration of intermediate **2** is the rate-determining step of path **A** for Pd-py^{t}bpx and in order to foresee whether the proton transfer in this step is affected by the basicity of pyridyl group, the effect of substituent at the 4-position of pyridyl rings on the dehydrative activity of palladium catalyst was predicted by computing the variation of **TS2-(py^{t}bpx-R)** on the free-energy surface. The outcomes displayed in Fig. 11 showed that introducing electron-donating substituent, such as methyl or methoxy group, at the *para*-position of pyridyl group would result to the rising of barrier. While, introducing electron-withdrawing chloric atom can boost the proton transfer and thus reduce barrier. This energy pattern predicts that the analogues of py^{t}bpx ligand bearing less-basic 4-substituted pyridyl group may exhibited higher dehydration activity.

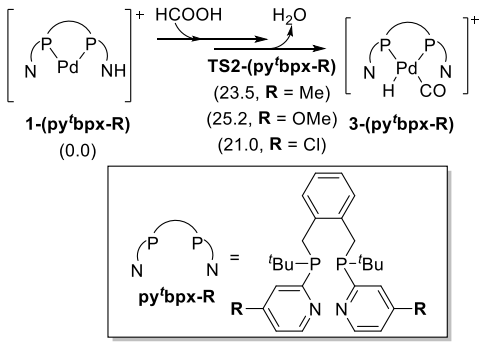

Figure 11 The free-energy variation of **TS2-(py^{t}bpx-R)** with the change of substituent at the 4-position of pyridine ring in py^{t}bpx ligand.

Conclusions

In summary, the DFT-based computational survey unveils the role of "built-in base" and strong *para*-toluenesulfonic acid promoter in the dehydrative decomposition of HCOOH to CO catalysed by Pd-py^{t}bpx. The basic pyridyl group installed in the ligand of py^{t}bpx changes the mode of intermolecular dehydration aid by the acid to the mode of intramolecular dehydration facilitated by the pyridinium group, which turns down the apparent activation energy of reaction. Excessive PTSA acid can lead to the bis-protonation of py^{t}bpx ligand, thereby further changes the selectivity of the product. Adding PTSA promoter, the activity of Pd-d^{t}bpx catalyst on HCOOH dehydration is enhanced, and the CO selectivity is also improved by inhibiting the H_2 production indirectly through transformaing the intermediate back to the active catalyst. Based on the hereby proposed mechanism, the positive effect of electron-withdrawing substituent at the *para*-position of pyridyl rings is predicted.

Author Contributions

C. S.: writing original draft, investigation, formal analysis, methodology, visualization; X. T.: review & editing conceptualization, methodology, project administration; Z. W.: review & editing; K. D.: conceptualization, funding acquisition. All the authors discussed the results and contributed to the writing of the manuscript.

Conflicts of interest

There are no conflicts to declare.

Acknowledgements

C.S. and X.T. thank the financial supports from the National Natural Science Foundation of China (No. 21903049 for X.T., 21802151 for C.S.) Part of the calculations were performed at the Shanghai Supercomputer Centre and the Supercomputing Centre of Shanxi University.

Notes and references

1 R. Sang, Y. Hu, R. Razzaq, R. Jackstell, R. Franke, M. Beller, *Org. Chem. Front.*, 2021, **8**, 799-811.

2 Z. Yin, J.-X. Xu, X.-F. Wu, *ACS Catal.*, 2020, **10**, 6510-6531.

3 J.-B. Peng, F.-P. Wu, X.-F. Wu, *Chem. Rev.*, 2019, **119**, 2090-2127.

4 X.-F. Wu, X. Fang, L. Wu, R. Jackstell, H. Neumann, M. Beller, *Acc. Chem. Res.*, 2014, **47**, 1041-105.

5 X.-F. Wu, H. Neumann, M. Beller, *Chem. Rev.*, 2013, 113, 1-35.

6 J. Pospech, I. Fleischer, R. Franke, S. Buchholz, M. Beller, *Angew. Chem. Int. Ed.*, 2013, **52**, 2852-2872.

7 A. Brennführer, H. Neumann, M. Beller, *Angew. Chem. Int. Ed. Engl.*, 2009, **48**, 4114-33.

8 S. D. Friis, A. T. Lindhardt, T. Skrydstrup, *Acc. Chem. Res.* 2016, **49**, 594-605.

9 Z. Chen, L.-C. Wang, X.-F. Wu, *Chem. Commun.*, 2020, **56**, 6016-6030.

10 L. Wang, W. Sun, C. Liu, *Chin. J. Chem.*, 2018, **36**, 353-362.

11 H. Konishi, *Chem. Pharm. Bull.* 2018, **66**, 1-19.

12 P. Gautama, B. M. Bhanage, *Catal. Sci. Technol.*, 2015, **5**, 4663-4702.

13 L. Wu, Q. Liu, R. Jackstell, M. Beller, *Angew. Chem. Int. Ed.*, 2014, **53**, 6310-6320.

14 L. R. Odell, F. Russo, M. Larhed, *Synlett*, 2012, 685-698.

15 T. Morimoto, K. Kakiuchi, *Angew. Chem. Int. Ed.*, 2004, **43**, 5580-5588.

16 F. Ramirez-Vega, P. Laurent, J.-C. Clément, H. des Abbayes *J. Mol. Catal. A: Chem.*, 1995, **96**, 15-20.

17 T. Ueda, H. Konishi, K. Manabe, *Angew. Chem. Int. Ed.*, 2013, **52**, 8611-8615.

18 L.-B. Jiang, X. Qi, X.-F. Wu, *Tetrahedron Lett.*, 2016, **57**, 3368-3370.

19 (a) J. S. Morgan, *J. Chem. Soc., Trans.*, 1916, **109**, 274-283; (b) R. E. DeRight, *J. Am. Chem. Soc.*, 1933, **55**, 4761-4764; (c) G. Ciuhandu, A. Dumitreanu, Z. Simon, *J. Prakt. Chem.*, 1976, **318**, 202-206.

20 J. Guo, C. K. Yin, D. L. Zhong, Y. L. Wang, T. Qi, G. H. Liu, L. T. Shen, Q. S. Zhou, Z. H. Peng, H. Yao, X. B. Li, *ChemSusChem*, 2021, **14**, 2655-2681.

21 J. Hou, J.-H. Xie Q.-L. Zhou, *Angew. Chem. Int. Ed.*, 2015, 54, 6302-6305.

22 J. Dai, W. Ren, W. Chang, P. Zhang, Y. Shi, *Org. Chem. Front.*, 2016, **3**, 1131-1136.

23 W. Liu, W. Ren, J. Li, Y. Shi, W. Chang, Y. Shi, *Org. Lett.*, 2017, **19**, 1748-1751.

24 W. Ren, J. Chu, F. Sun, Y. Shi, *Org. Lett.*, 2019, **21**, 5967-5970.

25 R. Sang, P. Kucmierczyk, K. Dong, R. Franke, H. Neumann, R. Jackstell, M. Beller, *J. Am. Chem. Soc.*, 2018, **140**, 5217-5223.

26 K. Dong, R. Sang, Z. Wei, J. Liu, A. Spannenberg, H. Jiao, R. Franke, M. Beller, *Chem. Sci.*, 2018, **9**, 2510-2516.

27 J. Liu, Z. Wei, J. Yang, Y. Ge, D. Wei, R. Jackstell, H. Jiao, M. Beller, *ACS Catal.*, 2020, **10**, 12167-12181.

28 M. J. Frisch, G. W. Trucks, H. B. Schlegel, G. E. Scuseria, M. A. Robb, J. R. Cheeseman, G. Scalmani, V. Barone, G. A. Petersson, H. Nakatsuji, X. Li, M. Caricato, A. V. Marenich, J. Bloino, B. G. Janesko, R. Gomperts, B. Mennucci, H. P. Hratchian, J. V. Ortiz, A. F. Izmaylov, J. L. Sonnenberg, D. Williams-Young, F. Ding, F. Lipparini, F. Egidi, J. Goings, B. Peng, A. Petrone, T. Henderson, D. Ranasinghe, V. G. Zakrzewski, J. Gao, N. Rega, G. Zheng, W. Liang, M. Hada, M. Ehara, K. Toyota, R. Fukuda, J. Hasegawa, M. Ishida, T. Nakajima, Y. Honda, O. Kitao, H. Nakai, T. Vreven, K. Throssell, J. A. Montgomery, Jr., J. E. Peralta, F. Ogliaro, M. J. Bearpark, J. J. Heyd, E. N. Brothers, K. N. Kudin, V. N. Staroverov, T. A. Keith, R. Kobayashi, J. Norm,, K. Raghavachari, A. P. Rendell, J. C. Burant, S. S. Iyengar, J. Tomasi, M. Cossi, J. M. Millam, M. Klene, C. Adamo, R. Cammi, J. W. Ochterski, R. L. Martin, K. Morokuma, O. Farkas, J. B. Foresman, D. J. Fox, Gaussian 16., Revision A.03.03, Gaussian, Inc., Wallingford C.T, 2016.

29 Y. Zhao, D. G. Truhlar, *Theor. Chem. Account.*, 2008, **120**, 215-241.

30 Y. Zhao, D. G. Truhlar, *Acc. Chem. Res.*, 2008, **41**, 157-167

31 F. Weigend, R. Ahlrichs, *Phys. Chem. Chem. Phys.* 2005, **7**, 3297-3305.

32 A. V. Marenich, C. J. Cramer, D. G. Truhlar, *J. Phys. Chem.* B 2009, **113**, 6378-6396.

33 T. Lu, Q. Chen, *Comput. Theor. Chem.*, 2021, **1200**, 113249.

34 L. C. Grabow, M. Mavrikakis, *ACS Catal.* 2011, 1, 365-384

35 R. Geitner, A. Gurinov, T. Huang, S. Kupfer, S. Grafe, B. M. Weckhuysen, *Angew. Chem. Int. Ed.*, 2021, **60**, 3422-3427

36 R. Sang, P. Kucmierczyk, R. Dühren, R. Razzaq, K. Dong, J. Liu, R. Franke, R. Jackstell, M. Beller, *Angew. Chem. Int. Ed.* 2019, **58**, 14365-14373

37 K. Dong, R. Sang, J. Liu, R. Razzaq, R. Franke, R. Jackstell , M. Beller, *Angew. Chem., Int. Ed.* 2017, **56**, 6203-6207.

38 J. Vondran, M. R. L. Furst, G. R. Eastham, Thomas Seidensticker, D. J. Cole-Hamilton, C*hem. Rev.*, 2021, **121**, 6610-6653

39 Q.-Y. Bi, J.-D. Lin, Y.-M. Liu, H.-Y. He, F.-Q. Huang, Y. Cao, *Angew. Chem. Int. Ed.*, 2016, **55**, 11849-11853.

40 H. J. Young, M. Chung, *App. Catal. B, Environ.*, 2017, **210**, 212-222.

41 Q. Wang, N. Tsumori, M. Kitta , Q. Xu, *ACS Catal.* 2018, **8**, 12, 12041-12045.

42 L. Di, J. Zhang, M. Craven, Y. Wang, H. Wang, X. Zhang, X. Tu, *Catal. Sci. Technol.*, 2020, **10**, 6129-6138.

43 S. Jones, S. M. Fairclough, M. Gordon-Brown, W. Zheng, A. Kolpin, B. Pang, W. C. H. Kuo, J. M. Smith, S. C. E. Tsang, *Chem. Commun.*, 2015, **51**, 46-49.

44 S. Zhang, B. Jiang, K. Jiang, W.-B. Cai, *ACS Appl. Mater. Interfaces*, 2017, **9**, 24678-24687.

45 Y. Kim, D. H. Kim, *App. Catal. B: Environ.*, 2019, **244**, 684-693.